Title: Osteopontin promotes survival of intestinal intraepithelial lymphocytes and protects against colitis

Authors: Ali Nazmi,[1] Michael J. Greer,[2] Kristen L. Hoek,[1] M. Blanca Piazuelo,[3] Joern-Hendrik Weitkamp,[4] and Danyvid Olivares-Villagómez[1,5,6]

[1]Department of Pathology, Microbiology and Immunology, Vanderbilt University Medical Center, A5301 Medical Center North, Nashville, Tennessee 37232, USA; [2]Department of Biomedical Informatics, Vanderbilt University, Nashville, Tennessee, 37232, USA; [3]Department of Medicine, Vanderbilt University Medical Center, 1030 MRBIV, Nashville, Tennessee 37232, USA; [4]Department of Pediatrics, Vanderbilt University Children's Hospital, 111111 Doctor's Office Tower, Nashville, Tennessee 37232, USA; [5]Vanderbilt Institute for Infection, Immunology and Inflammation, Vanderbilt University Medical Center, A5301 Medical Center North, Nashville, Tennessee 37232, USA; [6]ORCID, 0000-0002-1158-8976.

Corresponding author: Danyvid Olivares-Villagómez, Department of Pathology, Microbiology and Immunology, Vanderbilt University Medical Center, A5301 Medical Center North, Nashville, Tennessee 37232, USA. Telephone, 615-936-0134; email, danyvid.olivares-villagomez@vumc.org

Ali Nazmi and Michael J. Greer contributed equally to this report.

Abstract

Intestinal intraepithelial lymphocytes (IEL) comprise a diverse population of cells residing in the epithelium at the interface between the intestinal lumen and the sterile environment of the lamina propria. Because of this anatomical location, IEL are considered critical components of intestinal immune responses. Indeed, IEL are involved in many different immunological processes ranging from pathogen control to tissue stability. However, maintenance of IEL homeostasis is incompletely understood. In this report we present evidence that osteopontin, a glycophosphoprotein with diverse roles in biomineralization, cell-mediated immunity, and inflammation, is important for maintaining normal levels of IEL. Mice in which the osteopontin gene (Spp-1) is disrupted present decreased levels of IEL subtypes, such as TCR$\alpha\beta$ and TCR$\gamma\delta$ IEL in the intestine, an effect not observed for lymphocytes in other immune compartments such as spleen or lamina propria, indicating an epithelium-specific effect. *In vitro* experiments show that mouse and human IEL survival is improved by culture with recombinant osteopontin. CD44, a ligand for osteopontin, is conspicuously expressed in IEL, including mucosal regulatory T cells. We present *in vitro* and *in vivo* evidence supporting a role for the osteopontin-CD44 interaction in IEL and regulatory T cell homeostasis, with implications in the development of intestinal inflammation.

Introduction

One of the largest immunological compartments in the body is comprised of intraepithelial lymphocytes (IEL), a group of immune cells interspaced between the monolayer of intestinal epithelial cells (IEC). IEL can be divided into two groups based on T cell receptor (TCR) expression.[1, 2, 3] TCR^+ IEL express αβ or γδ chains. $TCR\alpha\beta^+$ IEL can be further subdivided into different populations such as $TCR\alpha\beta^+CD4^+$, $TCR\alpha\beta^+CD4^+CD8\alpha\alpha^+$, $TCR\alpha\beta^+CD8\alpha\beta^+$, and $TCR\alpha\beta^+CD8\alpha\beta^+CD8\alpha\alpha^+$ cells. TCR^{neg} IEL comprise innate lymphoid cells (ILC) [4, 5, 6] and lymphocytes characterized by expression of intracellular CD3γ chains ($iCD3^+$), some of which express CD8αα (iCD8α cells).[7, 8]

Because of their anatomical location, IEL function as sentinels between the antigenic contents of the intestinal lumen and the sterile environment under the basal membrane of the epithelium. Indeed, TCRγδ IEL surveil for pathogens,[9] secrete antimicrobials conferring protection against pathobionts,[10] and protect from intestinal inflammation.[11] TCRγδ IEL are also involved in protecting the integrity of damaged epithelium after dextran sodium sulphate (DSS)-induced colitis,[12] and are responsible, along with other IEL, for preserving IEC homeostasis.[13, 14] Other IEL, such as conventional effector CD8 T cells that migrate into the epithelium, can protect against *Toxoplasma* infection,[15] and reside in this organ as memory cells.[16, 17] IEL such as $TCR\alpha\beta^+CD4^+CD8\alpha\alpha^+$ cells can prevent development of colitis in an adoptive transfer model.[18] TCR^{neg} IEL such as iCD8α cells confer protection against *Citrobacter rodentium* infection and may protect against necrotizing enterocolitis in neonates,[8] but these cells can also promote intestinal inflammation in some experimental conditions.[19] $iCD3^+$ IEL are involved in malignancies associated with celiac disease.[7]

Osteopontin is a glycosylated phosphoprotein, encoded by the Spp-1 gene, originally characterized as part of the rat bone matrix.[20, 21] Osteopontin is a versatile molecule involved in many physiological processes, that include immunological roles, such as macrophage chemotaxis,[22] induction of Th1 responses,[23] suppression of T cell activated-induced cell death,[24] inhibition of natural killer (NK) cell apoptosis and promotion of NK cell responses,[25] and modulation of dendritic cell function.[26] The role of osteopontin during intestinal inflammation is diverse. For example, Spp-1-deficient mice present with milder disease in the trinitrobenzene sulphonic acid [27] and DSS models of

colitis.[28] In humans with inflammatory bowel diseases (IBD), plasma osteopontin is significantly increased as compared to normal individuals.[29, 30] Some reports indicate that osteopontin is downregulated in the mucosa of Crohn's disease (CD) patients,[31] whereas other groups have reported higher osteopontin expression in the intestines of individuals with CD and ulcerative colitis (UC) compared with healthy controls.[29, 32] Because of its potential involvement in IBD, this molecule could be a potential biomarker for IBD,[33] and has been explored as a potential therapeutic target in clinical trials.[34] These reports clearly underscore the importance of osteopontin in intestinal inflammation and warrant further investigation of this molecule in mucosal immune responses.

Recently, it was reported that the frequency and number of TCR$\gamma\delta$ IEL were reduced in osteopontin-deficient mice, while TCR$\alpha\beta$ IEL numbers remained similar in comparison to wild type controls.[35] However, *in vitro* neutralization of IEL-derived osteopontin resulted in decreased survival of TCR$\gamma\delta$ and TCR$\alpha\beta$ IEL,[35] confounding the *in vivo* results. Moreover, because of the IEL diversity present in the intestine, more detailed analysis is required to determine the survival requirements of different IEL populations. Herein, we provide substantial *in vitro* and *in vivo* evidence indicating that osteopontin promotes the survival of TCR$\gamma\delta$ and TCR$\alpha\beta$ IEL, including subpopulations of these cells, such as: TCR$\alpha\beta^+$CD4$^+$, TCR$\alpha\beta^+$CD4$^+$CD8$\alpha\alpha^+$ and TCR$\alpha\beta^+$CD8$\alpha\alpha^+$ cells. We also show that the survival effect is not only confined to murine IEL, but osteopontin also promotes the survival of human IEL. Additionally, osteopontin promotes a pro-apoptotic transcriptional profile, underscoring its role as a survival stimulus. Moreover, we show that the effect of osteopontin in IEL survival is mediated by CD44, a known receptor for osteopontin conspicuously expressed by IEL and regulatory T cells in the intestinal mucosa. Lastly, using two different models of intestinal inflammation, we present evidence indicating that the lack of osteopontin results in increased disease susceptibility.

Results

Osteopontin-deficient mice contain a reduced IEL compartment.

To determine the role of osteopontin in IEL homeostasis, we analyzed the IEL compartment of wild-type (WT) and Spp-1$^{-/-}$ mice. Flow cytometry studies revealed a reduction in the proportion of total IEL in the small intestine of Spp-1$^{-/-}$ mice compared with WT mice (Fig. 1a, FSC vs SCC dot plots). The percentages of certain TCRβ^+ IEL subpopulations, such as TCRβ^+CD4$^+$ and TCRβ^+CD4$^+$CD8$\alpha\alpha^+$ were reduced in Spp-1$^{-/-}$ mice, whereas others, such as TCRβ^+CD8$\alpha\alpha^+$ cells were similar among both groups of mice (Fig. 1a dot plots). The percentages of TCR$\gamma\delta^+$ and TCR^{neg} IEL, such as iCD8α cells, were similar between WT and Spp-1$^{-/-}$ mice. In terms of total cell numbers, Spp-1$^{-/-}$ mice presented a significant decrease in TCR$\gamma\delta^+$ IEL, corroborating the observations made by others (Fig 1a graphs).[35] However, we observed total cell number reduction in TCRβ^+ IEL due to the decline of TCRβ^+CD4$^+$, TCRβ^+CD8α^+ and TCRβ^+CD4$^+$CD8α^+ in the small intestine IEL of osteopontin-deficient mice. The numbers of TCR^{neg} IEL and the subpopulation iCD8α cells were similar among WT and Spp-1$^{-/-}$ mice (Fig 1a graphs). While colon IEL numbers from Spp-1$^{-/-}$ mice showed a similar pattern as in the small intestine, the numbers of TCR^{neg} IEL from these mice were significantly reduced as compared with WT mice (Fig. 1b). Interestingly, osteopontin-deficiency did not affect spleen T lymphocytes (Fig. 1c), or lamina propria CD19$^+$, TCRβ^+CD4$^+$ and TCRβ^+CD8$^+$ cells (Fig. 1d), suggesting that the major influence of this molecule is confined to the intestinal IEL compartment.

Increased apoptosis and decreased cellular division in IEL from osteopontin-deficient mice.

To investigate whether the reduction in IEL numbers in Spp-1$^{-/-}$ mice was due to increased cell death, we determined the levels of early/late apoptosis and necrosis. As shown in Fig. 2a, all IEL populations isolated from WT and Spp-1$^{-/-}$ mice analyzed presented similar levels of cells in early apoptosis (annexin V$^+$7AAD^{neg}). We observed a significantly higher percentage of late apoptotic (annexin V$^+$7AAD$^+$) TCR$\gamma\delta^+$ and TCRβ^+CD4$^+$CD8α^+, and a near significant higher percentage of TCRβ^+CD4$^+$ IEL from

Spp-1$^{-/-}$ mice. Because the cell death and proliferation rates are inversely related, we investigated the proliferation frequencies in different IEL populations. TCRβCD4^{+}, TCRβCD4^{+}CD8α^{+} and TCRβ^{+}CD8αα^{+} IEL derived from Spp-1$^{-/-}$ mice presented lower levels of dividing cells as indicated by the expression of Ki67 (Fig. 2b), corroborating the increase in apoptosis observed in IEL from osteopontin-deficient mice. However, despite the numbers of TCRγδ IEL were reduced in Spp-1$^{-/-}$ mice and presented an increased frequency of cells in late apoptosis, TCRγδ IEL from Spp-1$^{-/-}$ mice showed similar proliferation levels as cells derived from WT mice.

Overall, these results show that in the absence of osteopontin, IEL present higher apoptosis and reduced cell proliferation, which may account for the decreased IEL numbers observed in osteopontin-deficient mice.

CD44 deficiency affects the IEL compartment.

CD44 is one of the receptors for osteopontin[36] and is also expressed by IEL (Fig. 3a). Therefore, we reasoned that if osteopontin provides a survival signal via CD44, the absence of this receptor should also result in decreased numbers of IEL. Most IEL populations from CD44$^{-/-}$ mice presented a trend of decreased numbers in both the small intestine and colon (Fig. 3b and 3c) in comparison to IEL from wild type mice. The difference was significant for total colon TCRβ^{+} and subpopulations such as TCRβ^{+}CD4^{+}, and TCRβ^{+}CD8αα^{+} IEL. Interestingly, TCR^{neg} cells also presented a reduction in numbers in the small intestine and colons of CD44$^{-/-}$ mice. These results show similarities between the IEL compartment observed in Spp-1$^{-/-}$ and CD44$^{-/-}$ mice, suggesting a role for the osteopontin-CD44 interaction for IEL survival.

As shown in Fig.1, the effect of osteopontin in steady-state levels seems to affect only the IEL compartment. To determine whether the frequencies of other CD44^{+} cells in other immune compartments are affected by oseteopontin, we analyzed TCRγδ^{+}, TCRαβ^{+}CD4^{+} and TCRαβ^{+}CD8^{+} T cells from the spleen. The fraction of CD44^{+} cells in these three populations was undistinguishable between WT and Spp-1$^{-/-}$ mice (Fig 3c), indicating that, at steady state levels, osteopontin does not affect the frequency of activated CD44^{+} spleen T cells.

Osteopontin promotes survival of IEL in a CD44-dependent manner.

To further investigate the role of osteopontin in IEL survival, we used an *in vitro* system. For this purpose, first, we isolated total IEL ($CD45^+$ cells from IEL preparations) from WT mice and cultured them under different conditions. $CD45^+$ IEL cultured in media alone resulted in ~30% cell survival after 24 h of culture, followed by a constant decrease thereafter. However, addition of recombinant osteopontin resulted in improved IEL survival, to around 50% 24 h post culture (Fig. 4a). Recombinant osteopontin maintained increased IEL survival compared with media alone at 48 and 72 h post culture. However, when IEL were cultured in the presence of recombinant osteopontin and anti-osteopontin antibodies, cell survival was blunted to levels similar as observed for media alone, indicating that IEL *in vitro* survival was mediated by recombinant osteopontin (Fig. 4a). IEL incubated only with anti-osteopontin antibodies behaved similarly as cells cultured in media alone, suggesting that under these experimental conditions either IEL did not produce osteopontin or IEL-derived osteopontin was not a factor in cell survival. These results are in contrast to the work of Ito et al., that showed that IEL-derived osteopontin was important for their *in vitro* survival;[35] differences in culture systems between the two groups may account for this discrepancy. To determine whether the observed osteopontin-mediated IEL survival was facilitated by CD44, IEL were cultured in the presence of recombinant osteopontin and anti-CD44 antibodies. As shown in Fig. 4a, CD44 blockage resulted in decreased IEL survival similar to that observed for media alone, especially at 48 and 72 h post-culture. Moreover, $CD45^+$ IEL derived from CD44-deficient mice cultured with recombinant osteopontin presented similar survival as IEL cultured in media alone (Fig. 4b), underscoring the importance of the interaction between osteopontin and CD44 in IEL survival. We then investigated the survival of different FACS-enriched IEL subpopulations from WT mice when cultured in the presence or absence of recombinant osteopontin. Increased survival was observed in $TCR\gamma\delta^+$, $TCR\beta^+CD4^+$, $TCR\beta^+CD8\alpha^+$ and $TCR\beta^+CD4^+CD8\alpha^+$ IEL when recombinant osteopontin was included in the media; however, the effect on survival was observed at different time points depending on the IEL population analyzed (Fig. 4c). Addition of anti-CD44 to the cultures blunted the osteopontin effect (Fig. 4c).

To determine whether osteopontin influences the survival of spleen T cells, we first incubated total splenocytes from WT mice in the presence or absence of recombinant osteopontin. As shown in Fig. 4d, survival of total spleen T cells was not affected by osteopontin. Moreover, FACS-enriched $TCR\beta^{+}CD44^{hi}$ spleen cells from WT and Spp-$1^{-/-}$ mice cultured in the presence or absence of osteopontin and/or anti-CD44 presented no difference in their survival (Fig. 4e), indicating that osteopontin preferentially influences the *in vitro* survival of IEL via CD44 but not of total or $CD44^{+}$ spleen T cells.

The immune system of mice maintained in specific pathogen-free conditions more closely resembles that of human neonates rather than adults.[37] Therefore, to determine whether our findings with murine IEL are relevant to humans, we isolated total IEL from human neonates and cultured them in the presence or absence of recombinant osteopontin. Human IEL survived better in the presence of recombinant osteopontin than in its absence, and addition of anti-CD44 blunted the cytokine effect (Fig. 4f), in parallel to the results observed with mouse IEL. To determine the effect of osteopontin on other human lymphocytes, we employed PBMC from healthy adults, as we were unable to obtain PBMCs from the same neonate individuals for this purpose. As shown in Figure 4g, PBMC survival was not enhanced or reduced by any of the treatments used, which corroborates an intestinal IEL specific effect. Our results indicate that osteopontin promotes survival of murine and human IEL, and at least in the mouse system, this effect is mediated by CD44.

Osteopontin induces a survival program in IEL

The *in vivo* and *in vitro* studies presented in the previous sections indicate that osteopontin is an important cytokine involved in the survival of IEL. To investigate whether osteopontin, or its absence, alters the IEL transcription profile, we isolated RNA from FACS-enriched $TCR\gamma\delta^{+}$, $TCR\beta^{+}CD4^{+}$, $TCR\beta^{+}CD8\alpha^{+}$ and $TCR\beta^{+}CD4^{+}CD8\alpha^{+}$ IEL derived from naïve WT and Spp-$1^{-/-}$ mice, and determined the expression of genes involved in preventing apoptosis. Comparison of genes expressed in IEL from WT and Spp-$1^{-/-}$ mice showed that $TCR\gamma\delta^{+}$ cells from WT animals had more differentially expressed anti-apoptotic genes in comparison to the other IEL populations (Fig. 5a).

TCRβ$^+$CD8α$^+$ IEL presented little differential expression among the anti-apoptotic genes analyzed. On the other hand, TCRβ$^+$CD4$^+$ and TCRβ$^+$CD4$^+$CD8α$^+$ IEL differentially expressed some of these genes (Fig. 5a). Birc2, a known inhibitor of apoptosis in malignancies,[38] was one of the genes consistently differentially expressed in most IEL analyzed from WT mice, including TCRβ$^+$CD4$^+$CD8α$^+$ cells (Fig. 5b). Other anti-apoptotic genes with higher expression in WT IEL were Prdx2, Polb, Dffa, Bric5 and Bcl10. Overall, these results indicate that osteopontin induces the expression of anti-apoptotic genes, but the gene profile varies between different IEL populations.

Because addition of recombinant osteopontin rescued wild type-derived CD45$^+$ IEL survival when cultured *in vitro* (Fig. 4a), we interrogated whether addition of this cytokine in cultured wild type IEL modifies their gene expression profile. For this purpose, we cultured FACS-enriched CD45$^+$ IEL from wild type mice in the presence or absence of osteopontin. Twenty-four hours post-culture, cells were collected, RNA extracted, sequenced and the gene expression profile determined. As recovery of sufficient cells for gene expression profile analysis after 24 h of culture from individual IEL populations was limiting, total CD45$^+$ IEL were used as an alternative approach. Gene set enrichment analysis (GSEA) revealed that IEL cultured in the presence of recombinant osteopontin express genes associated with retinoid X receptor (RXR) functions (Fig. 5c and 5d). This set included genes encoding products such as the vitamin D receptor (VDR), which dimerizes with RXR and modulates osteopontin gene transcription by binding to its promoter region,[39] and may induce a feedback loop in osteopontin-expressing IEL. GSEA also showed that IEL cultured in media alone present enriched pathways related to apoptosis, degradation of p27/p21 and downregulation of genes in Tregs (Fig. 5c and 5d). These sets included genes coding for proteasomal subunits, genes associated with cell cycle regulation (cyclin a2 and e1), and genes involved in programmed cell death pathways such as, caspases, Uba52, and Maged1. These results indicate that *in vitro* IEL exposure to osteopontin has an impact on the IEL gene transcription profile. However, it is important to consider that use of total CD45$^+$ IEL as the source for RNA increases variability in the results due to the different IEL populations present in the CD45$^+$ compartment.

Osteopontin serves as checkpoint for development of intestinal inflammation

We reasoned that if osteopontin deficiency affects the IEL compartment, and proper homeostasis of these cells is critical for protection against inflammation, then Spp-1$^{-/-}$ mice may be susceptible to spontaneous intestinal inflammation. For these purposes we monitored female Spp-1$^{-/-}$ mice from the time of weaning until 32 weeks of age. These mice gained weight during the observation period but not as much as wild type control females (Fig. 6a) and presented normal small intestine (Fig. 6b) and colon (not shown) architecture without signs of inflammation. However, spontaneous inflammation may become evident if another molecule involved in IEL homeostasis is disrupted. For this purpose, we crossed Spp-1$^{-/-}$ mice with thymus leukemia (TL) antigen deficient mice. TL is expressed in IEC and preferentially binds to CD8$\alpha\alpha$ homodimers on IEL, controlling their effector functions and proliferation.[40] While TL-deficient animals do not develop spontaneous intestinal inflammation, when crossed to a susceptible strain, the offspring present an early onset and increased incidence of spontaneous intestinal inflammation.[41] Therefore, it is possible that disruption of two systems involved in IEL homeostasis, the TL-CD8$\alpha\alpha$ and the osteopontin-CD44, may result in spontaneous intestinal inflammation. Spp-1$^{-/-}$TL$^{-/-}$ mice also gained weight during all the observation period but at lower levels than WT and Spp-1$^{-/-}$ mice (Fig. 6a; for figure clarity, statistical significance at the relevant time points is presented in the figure legend). Interestingly, analysis of ileum pathology showed an increase in IEL and lamina propria inflammatory foci in Spp-1$^{-/-}$TL$^{-/-}$ in comparison to WT and Spp-1$^{-/-}$ mice (Fig. 6b and 6c). These results indicate that in the proper context, the absence of osteopontin may lead to spontaneous intestinal inflammation, underscoring its importance as an intestinal checkpoint.

Osteopontin prevents intestinal inflammation but not migration into the epithelium.

We have provided evidence indicating that the IEL deficiency observed in Spp-1$^{-/-}$ mice is due to IEL survival; however, it is possible that osteopontin also affects migration of T cells into the epithelium. To test this hypothesis, we adoptively transferred total spleen T cells from WT mice into Rag-2$^{-/-}$ or Spp-1$^{-/-}$Rag-2$^{-/-}$ recipient mice, and after 7 days we determined the number of cells migrating into the intestinal

epithelium. Both TCRβ^{+}CD4^{+} and TCRβ^{+}CD8α^{+} cells migrated similarly into the epithelium of Rag-2$^{-/-}$ or Spp-1$^{-/-}$Rag-2$^{-/-}$ recipient mice (Fig. 7a), indicating that osteopontin does not influence the migration of these cells into the intestinal mucosa. We did not analyze spleen-derived TCRγδ cells because their numbers in the inoculum were very low and these cells do not reconstitute the mucosa properly. Interestingly, reconstitution analysis at 28 days post transfer showed a reduction in the total number of TCRβ^{+}CD4^{+} and TCRβ^{+}CD4^{+}CD8α^{+} cells (Fig. 7b), which resembled what was observed in Spp-1-deficient mice (Fig. 1a). On the other hand, the numbers of adoptive transferred TCRβ^{+}CD8α^{+} cells recovered were similar between Rag-2$^{-/-}$ or Spp-1$^{-/-}$Rag-2$^{-/-}$ recipient mice at 28 days post transfer (Fig. 7b). To prevent the development of intestinal inflammation in Rag-2$^{-/-}$ recipient mice, we transferred total T cells, which includes regulatory T cells. To our surprise, Spp-1$^{-/-}$Rag-2$^{-/-}$ recipient mice lost more weight than Rag-2$^{-/-}$ mice (Fig. 7c) and presented increased colon inflammation (Fig. 7d), suggesting that the absence of osteopontin in the host promoted disease development. To test whether CD44, as a receptor for osteopontin, was also involved in disease development in this system, we adoptively transferred total T cells from CD44$^{-/-}$ donor mice into Rag-2$^{-/-}$ and Spp-1$^{-/-}$Rag-2$^{-/-}$ recipient mice. Rag-2$^{-/-}$ mice that received total spleen T cells from WT mice did not lose weight, whereas Rag-2$^{-/-}$ and Spp-1$^{-/-}$Rag-2$^{-/-}$ recipient mice that received spleen cells from CD44$^{-/-}$ donor mice lost weight comparably starting at 2 weeks post transfer (Fig. 7e), with clear signs of intestinal inflammation (Fig. 7f).

Overall, this evidence indicates that adoptive transfer of total T cells into Spp-1$^{-/-}$ Rag-2$^{-/-}$ mice result in similar TCRβ^{+}CD4^{+} and TCRβ^{+}CD8α^{+} T cell migration into the IEL compartment at 7 days after transference; however, the total number of TCRβ^{+}CD4^{+} and TCRβ^{+}CD4^{+}CD8α^{+} T were significantly reduced in an osteopontin-deficient environment. Unexpectedly, decreased IEL reconstitution was accompanied by intestinal inflammation. These results suggest that host-derived oseopontin and expression of CD44 on the transferred T cells, are important for preventing development of intestinal inflammation even in the presence of regulatory T cells.

Osteopontin sustains Foxp3 expression in Tregs

We expected that transferring total T cells into Spp-1$^{-/-}$Rag-2$^{-/-}$ mice would result in protection against intestinal inflammation similar to that observed for Rag-2$^{-/-}$ recipient mice, due to the presence of regulatory T cells in the inoculum. However, because disease was observed in Spp-1$^{-/-}$Rag-2$^{-/-}$ recipient mice, we investigated the fate of regulatory T cells in the presence or absence of osteopontin. Regulatory T cells are known to express CD44, which when ligated, promotes sustained Foxp3 expression.[42] Thus, we hypothesized that binding of osteopontin to CD44 is a potential signal that maintains proper Foxp3 expression. To test this possibility, we cultured CD4 T cells derived from the intestinal mucosa from RFP-Foxp3 mice in the presence or absence of recombinant osteopontin, with or without anti-CD44. After 72 h of culture, there was an increase in the percentage of RFP^{+} cells in the presence of osteopontin, which was blunted with the addition of anti-CD44 antibodies (Fig. 8a). Figure 8b shows the combined fold increase over the untreated cells.

To test whether osteopontin sustains Foxp3 expression *in vivo*, we sorted splenic RFP^{+} cells from RFP-Foxp3 reporter mice and adoptively transferred them into Rag-2$^{-/-}$ or Spp-1$^{-/-}$Rag-2$^{-/-}$ recipient mice. Eight weeks after transfer, IEL were isolated and the percentage of donor-derived (CD45^{+}TCRβ^{+}CD4^{+}) RFP^{+} cells was determined (Fig. 8c, dot plots). Rag-2$^{-/-}$ mice presented a trend of higher percentage of donor-derived cells in the IEL compartment than Spp-1$^{-/-}$Rag-2$^{-/-}$ recipient mice (Fig 8d). Approximately 10% of the donor-derived cells from Rag-2$^{-/-}$ recipient mice remained RFP^{+}, whereas only 4% of cells recovered from Spp-1$^{-/-}$Rag-2$^{-/-}$ recipient mice remained RFP^{+} (Fig. 8e). These results indicate that osteopontin sustains Foxp3 expression in regulatory T cells in the IEL compartment, possible mediated by CD44 ligation, with significant impact in the development of intestinal inflammation.

Discussion

Intestinal IEL reside in the unique environment of the IEC monolayer. In this anatomical location, IEL are poised as the first immunological layer of defense against potential pathogens from the intestinal lumen. In order for IEL to fulfill their immunological roles, they need to remain in their niche and survive. However, because IEL represent a diverse population of lymphoid cells, requirements for their homeostasis within the

epithelium may depend on the particular type of IEL. For example, TCRγδ$^+$ IEL require IL-7 for their proper development whereas other IEL are not affected by this cytokine.[43] On the other hand, IL-15 deficiency does not disturb TCRγδ$^+$ IEL but has a significant impact on TCRαβ$^+$CD8αα$^+$, iCD8α and iCD3$^+$ IEL.[7, 8, 44] The results presented in this report indicate that osteopontin provides survival signals to a great fraction of IEL, including TCRαβ, TCRγδ and TCR^{neg} cells. This implies that despite having different developmental pathways and cytokine requirements, the presence of osteopontin in the epithelium ensures the survival of most types of intestinal IEL.

Osteopontin-mediated T cell survival has been documented previously. For example, concanavalin A-activated T cells from lymph nodes show reduced levels of cell death in the presence of osteopontin.[24] Moreover, Hur et al. also demonstrated that osteopontin alters the expression of pro-apoptotic molecules such as Bim, Bak and Bax, promoting T cell survival.[24] Using an *in vitro* system, we showed that TCR$^+$ IEL rapidly die in the absence of osteopontin, whereas IEL cultured in the presence of osteopontin presented increased *in vitro* survival (Fig. 4). It is important to notice the differential behavior of cultured IEL subpopulations, e.g., the survival of TCRγδ$^+$ and TCRβ$^+$CD4$^+$CD8α$^+$ IEL is less than 50% after 24 h post culture decreasing to around 10% by 72 h, and it is at this point that the effect of osteopontin is more evident for these cells. On the other hand, TCRβ$^+$CD4$^+$ and TCRβ$^+$CD8α$^+$ IEL have a better survival after 24 h (more than 50%), whereas the osteopontin effect is evident for the former cells starting at 48 h. These results indicate that each IEL subpopulation possess different survival kinetics, but appear to have a similar requirement for osteopontin for their survival.

Because IEL are considered to be in a “semi-activated” state,[45] osteopontin appears to primarily affect activated T cells, which express CD44. Interestingly, splenic CD44$^+$ T cell numbers are similar in wild type and Spp-1$^{-/-}$ mice (Fig. 3c), suggesting that osteopontin does not affect the overall effector T cell population. Moreover, *in vitro* survival of CD44$^+$ spleen T cells is not affected by addition of osteopontin (Fig. 4e). It is important to note that previous reports have demonstrated a pivotal role for osteopontin as an enhancer for the survival of effector Th17 cells, particularly during brain

inflammation;[24] however, whereas this group studied differentiated Th17 cells in the context of brain inflammation our results are based on $CD44^+$ T cells in naïve animals.

In the adoptive transfer experiments reported here, donor CD4 T cells from wild type mice reconstituted the IEL compartment of Spp-$1^{-/-}$Rag-$2^{-/-}$ recipient mice less efficiently than in Rag-$2^{-/-}$ recipient mice (Fig. 7), suggesting that an environment capable of producing osteopontin is important for proper cell survival. However, transfer of T cells from osteopontin-deficient donor mice into Rag-$2^{-/-}$ recipient mice resulted in reduced survival rates in the spleen and lymph nodes in comparison to donor T cells from wild type donor mice.[25] These results indicate that intrinsic T cell-derived osteopontin is critical for normal cell reconstitution in secondary lymphoid organs whereas T cells present in the IEL compartment present an increase dependency for their survival on osteopontin derived from the environment.

Adoptive transfer of total spleen T cells into immunodeficient hosts, such as Rag-$2^{-/-}$ mice, results in cellular reconstitution and protection from T cell-mediated colitis due to the presence of regulatory T cells.[46, 47] Surprisingly, when recipient Rag-$2^{-/-}$ mice were deficient in osteopontin (Rag-$2^{-/-}$Spp-$1^{-/-}$ animals), mice developed colitis even in the presence of regulatory T cells, indicating that environmental osteopontin is important for maintaining regulatory T cell function (Fig. 7). This was evident when transfer of regulatory T cells (RFP-$Foxp3^+$ cells) into Spp-$1^{-/-}$Rag-$2^{-/-}$ hosts resulted in lower recovery of RFP^+ cells from the intestinal epithelium in comparison to cells transferred into Rag-$2^{-/-}$ hosts (Fig. 8c and d). Therefore, similar to other IEL, regulatory T cells appear to be responsive to osteopontin via CD44, but in this case osteopontin helps to sustain the levels of Foxp3 expression. Of note, activation of naïve T cells ($CD4^+CD45RB^{hi}$) or their subsequent pathogenic capacity when adoptively transferred into Rag-$2^{-/-}$ mice requires T cell-derived osteopontin.[48]

If a significant fraction of IEL require osteopontin for their survival, what are the cellular sources for this cytokine in the intestines? Under steady-state conditions IEC do not express osteopontin, but some IEL populations do. Osteopontin expression appears to be confined to TCR$\gamma\delta$ and TCR$\alpha\beta^+CD8\alpha^+$ IEL.[35] On a per cell basis, iCD8α cells present high levels of osteopontin mRNA expression.[8] Therefore, IEL survival may

depend on IEL-derived osteopontin, suggesting possible interactions between different IEL populations.

In the past few years, the role of osteopontin in the etiology of human diseases has been greatly appreciated. For example, recent work has investigated the use of neutralizing anti-osteopontin antibodies as a therapeutic with preclinical studies currently underway (ref. in [49]). Studies such as the one described herein show that osteopontin neutralization may carry unwanted side-effects, especially if patients are immunocompromised. Osteopontin appears to be a critical molecule with multiple effects, one of them supporting proper IEL homeostasis, and therefore additional studies are needed to better understand its function and how it affects the biology of the mucosal immune system.

Figure legends

Fig. 1. Spp-1$^{-/-}$ mice have a deficient IEL compartment. **a** Representative frequency (dot plots) and total cell numbers (graphs) of different IEL populations from the small intestine of wild type (WT) and Spp-1$^{-/-}$ mice. After excluding dead cells (not shown) and IEC, cells were gated as CD45^{+} cells (not shown). Each dot represents an individual mouse (n = 12). **b** Total IEL numbers from colon of WT and Spp-1$^{-/-}$ mice, gated as in **a.** Each dot represents an individual mouse (n = 13). **c** Total cell numbers of the indicated populations in spleen from WT and Spp-1$^{-/-}$ mice (n=8). Bars indicate SEM. **d** Total cell numbers of different lymphoid populations in the lamina propria**.** Each dot represents an individual mouse (n=5). Data from **a** to **d** are representative of two to three independent experiments. * P<0.05; ** P<0.01; *** P<0.001; **** P<0.0001 (Mann-Whitney U test).

Fig. 2. IEL from osteopontin-deficient mice present higher apoptosis and less cell division. **a** Annexin V staining of different IEL populations derived from WT and Spp-1$^{-/-}$ mice. Cells were gated as CD45^{+} cells. Dot plots show a representative sample. Summary is indicated in the graphs. Early apoptosis (annexin V^{+}7AAD^{neg}), late apoptosis (annexin V^{+}7AAD^{+}), necrosis (annexin V^{neg}7AAD^{+}). Data are representative of three independent experiments. Each dot represents an individual sample (n = 8 to 10).

b Ki67 intracellular staining of different IEL populations derived from WT and Spp-1$^{-/-}$ mice. After excluding dead cells and IEC, cells were gated as CD45^{+} cells. Data are representative from two independent experiments. Each dot represents an individual sample (*n* = 9 to 10). **P*<0.05; ***P*<0.01 (Mann-Whitney U test).

Fig. 3. CD44$^{-/-}$ mice have a reduced IEL compartment. **a** CD44 expression in TCR$\gamma\delta^{+}$ and TCRβ^{+} IEL from WT mice. After excluding dead cells and IEC, cells were gated as CD45^{+} cells. **b** Total numbers of different IEL populations derived from the small intestine or colon from WT and CD44$^{-/-}$ mice. Data is combined of three independent experiments (*n* = 12 to 19). **c** CD44 expression in the indicated spleen T cells from WT and Spp-1$^{-/-}$ mice. After excluding dead cells, cells were gated as CD45^{+} cells. Dot plots show a representative sample. Results are summarized in graphs. Data are representative from two independent experiments. Each dot represents an individual sample (*n* = 9 to 10). **P*<0.05 (Mann-Whitney U test).

Fig. 4. Osteopontin promotes IEL survival. **a** Enriched total CD45^{+} IEL from WT mice were incubated in the presence or absence of anti-mouse osteopontin (2 μg/ml), recombinant murine osteopontin (2 μg/ml), and anti-mouse CD44 (5 μg/ml). After the indicated time points, cell survival was determined. Data are representative of three independent experiments. Biological replicates consisted of two to three independent pooled IEL preparations from individual mice; each experiment consisted of 3 biological replicas. **b** Enriched total CD45^{+} IEL from CD44$^{-/-}$ mice were treated as in **a**. Data are representative of three independent experiments. Biological replicas consisted of two to three independent pooled IEL preparations from individual mice; each experiment consisted of 3 biological replicas. **c** Indicated FACS-enriched IEL populations from WT mice were left untreated or treated with recombinant osteopontin with or without anti-CD44. After the indicated time points, cell survival was determined. Data are representative of three independent experiments. Biological replicas consisted of two to three independent pooled IEL preparations from individual mice; each experiment consisted of 3 biological replicas. **d** Enriched CD45^{+} splenocytes were incubated in the presence or absence of recombinant osteopontin (2 μg/ml). After the indicated time

476 points, cell survival was determined. Data are representative of two independent
477 experiments (*n* = 3). **e** FACS-enriched TCRβ^{+}CD44^{+} spleen cells from WT and Spp-1$^{-/-}$
478 mice were treated as in **c**. After the indicated time points, cell survival was determined.
479 Data are representative of two independent experiments (*n* = 3). **f** Neonatal human IEL
480 were incubated in the presence or absence of recombinant human osteopontin (2
481 μg/ml) and anti-human CD44 (5μg/ml). After the indicated time points, cell survival was
482 determined. Each symbol represents an individual human: circle, small intestine from 1-
483 day old patient presenting volvulus and necrosis; square, ileum and colon from 17-day
484 old patient presenting necrotizing enterocolitis; triangle, jejunum from 12-day old patient
485 presenting necrotizing enterocolitis; diamond and hexagon, de-identified individuals. **g**
486 PBMC from adult humans were incubated in the presence or absence of recombinant
487 human osteopontin with or without anti-human CD44 (5 μg/ml). After the indicated time
488 points, cell survival was determined. Data are representative of two independent
489 experiments (*n* = 3). **P*<0.05; ***P*<0.01; ****P*<0.001; *****P*<0.0001 (One-way ANOVA).
490 aOPN = anti-osteopontin antibody; rOPN = recombinant osteopontin; aCD44 = anti-
491 CD44 antibody.
492
493 **Fig. 5.** Osteopontin induces a survival program in IEL. **a** RNA was isolated from FACS-
494 enriched TCRγδ^{+}, TCRβ^{+}CD4^{+}, TCRβCD8α^{+} and TCRβ^{+}CD4^{+}CD8α^{+} IEL from WT and
495 Spp-1$^{-/-}$ mice, and used to detect expression of anti-apoptosis-related genes using a
496 QIAGEN RT^{2} Profiler PCR Array. Each column represents the average of 4 samples
497 from individual mice. Heat-map is a representative experiment of two performed. **b**
498 Heat-map representing a sample of genes differentially expressed in most WT IEL
499 populations. Data were derived from (**b**). **c** Enriched CD45^{+} IEL derived from 2
500 individual WT mice were pooled into one biological replicate. A total of 8 mice were
501 used yielding 4 replicates. Half the cells from each replicate were incubated in the
502 presence or absence of osteopontin (2 μg/ml) for 24 h. RNA-Seq was used to detect
503 gene expression profile. Each column depicts a representative biological replicate. **c**
504 Gene set enrichment analysis summary.
505

Fig. 6. Combined osteopontin and TL deficiency results in spontaneous ileal inflammation. **a** Weights of WT, Spp-1$^{-/-}$ and Spp-1$^{-/-}$TL$^{-/-}$ female mice were monitored for seven months starting at weaning age (*n* = 3 to 5). Statistical difference for: WT vs Spp-1$^{-/-}$ mice was *P*<0.05 or *P*<0.01 between week 6 to 24; WT vs Spp-1$^{-/-}$TL$^{-/-}$ mice was *P*<0.005 or *P*<0.001 between week 6 to 32; and Spp-1$^{-/-}$ vs Spp-1$^{-/-}$TL$^{-/-}$ mice was *P*<0.01 only at week 30 (two-way ANOVA). **b** Representative H&E sample of ileum at the end time point (200X magnification). Ovals indicate foci of IEL and lamina propria inflammation. Arrows indicate lymphocyte infiltration. **c** Summary of pathology score. Each symbol represents an individual sample.

Fig. 7. Environmental osteopontin influences IEL reconstitution and prevents intestinal inflammation. **a** Enriched total spleen T cells from WT mice were adoptively transferred into the indicated recipients mice, and 7 days after transfer, donor-derived cells were analyzed. After excluding dead cells, donor cells were gated as TCRβ^+CD45$^+$ IEL. Dot plots show a representative sample. Results are summarized in graphs. TCRβ^+CD4$^+$CD8α^+ cells were not detected above background at this time point in either group. Data are representative from two independent experiments. Each dot represents an individual sample (*n* = 4 to 5). **b** The same analysis as in (**a**) performed at 28 days post transfer. After excluding dead cells, donor cells were gated as TCRβ^+CD45$^+$ IEL (not shown). Dot plots show one representative sample. Results are summarized in graphs. Data are representative from three independent experiments. Each dot represents an individual animal (*n* = 9). **c** Total weight change at 28 days post transfer of mice treated as in **b**. Data are representative from three independent experiments. Each dot represents an individual sample (*n* = 9). **d** Representative H&E stained samples of colon sections from the indicated mice analyzed at 28 days of (200X magnification). Graph indicates total histological score [immune cell infiltration (3 points), loss of goblet cells (3 points), crypt damage (3 points) and epithelial hyperplasia (3 points)]. Data are representative from three independent experiments. Each dot represents an individual sample (*n* = 9). **e** Enriched total T cells from CD44$^{-/-}$ mice were adoptively transferred into the indicated recipient mice and weights were monitored weekly. **f** Colon pathology scored as in (**d**). Data are representative from two

537 independent experiments. Each dot represents an individual sample (*n* = 6 to 7).
538 ***P*<0.01 (Mann-Whitney U test).
539
540 **Fig. 8**. Osteopontin sustains Foxp3 expression. **a** Intestinal T cells from RFP-Foxp3
541 reporter mice were isolated and cultured in the presence or absence of recombinant
542 osteopontin (2 μg/ml) and anti-CD44 (5 μg/ml). Seventy-two hours later, the percentage
543 of RFP^+ cells was determined by flow cytometry. After excluding dead cells, dot plots
544 were gated as $CD45^+TCR\beta^+$ cells. **b** Bar graph indicates the fold change in $CD4^+RFP^+$
545 cells in relation to the null group. Data are representative of three independent
546 experiments. **c** Enriched splenic RFP^+ cells from RFP-Foxp3 reporter mice were
547 adoptively transferred into Rag-$2^{-/-}$ and Spp-$1^{-/-}$Rag-$2^{-/-}$ recipient mice. Eight weeks after
548 transfer, IEL from small intestine were isolated and the percentage of RFP^+ determined.
549 After excluding dead cells, dot plots were gated as indicated by the arrows. **d** Summary
550 of the percentage of donor-derived cells recovered; each dot represents an individual
551 mouse. Data are representative from three independent experiments. **e** Summary of the
552 percentage of RFP^+ cells within the donor-derived cells. **P*<0.05 (Mann-Whitney T
553 test). rOPN = recombinant osteopontin; aCD44 = anti-CD44 antibodies.
554
555 **Materials and Methods**
556 *Mice*. $CD44^{-/-}$, Rag-$2^{-/-}$, Spp-$1^{-/-}$ and RFP-Foxp3 reporter mice on the C57BL/6
557 background were obtained from the Jackson Laboratories. $TL^{-/-}$ mice were developed in
558 our laboratory as previously described.[41] To homogenize the microbiome of vendor-
559 derived mice, we co-housed or bred mice with established WT C57BL/6 mice from our
560 colony. Spp-$1^{-/-}$Rag-$2^{-/-}$ mice were generated in our colony by breeding Spp-$1^{+/-}$ with
561 Rag-$2^{+/-}$ mice. Spp-$1^{-/-}TL^{-/-}$ mice were generated in our colony by breeding Spp-$1^{+/-}$ with
562 $TL^{+/-}$ mice. Mice were maintained in accordance with the Institutional Animal Care and
563 Use Committee at Vanderbilt University.
564
565 *IEL isolation*. IEL were isolated by mechanical disruption as previously reported.[41]
566 Briefly, after flushing the intestinal contents with cold HBSS and removing excess
567 mucus, the intestines were cut into small pieces (~1cm long) and shaken for 45 minutes

568 at 37°C in HBSS supplemented with 5% fetal bovine serum and 2 mM EDTA.
569 Supernatants were recovered and cells isolated using a discontinuous 40/70% Percoll
570 (General Electric) gradient. To obtain lamina propria lymphocytes, intestinal tissue was
571 recovered and digested with collagenase (187.5 U/ml, Sigma) and DNase I (0.6 U /ml,
572 Sigma). Cells were isolated using a discontinuous 40/70% Percoll gradient.
573
574 *Human samples.* The Vanderbilt University Medical Center Institutional Review Board
575 approved sample collection (IRB# 090161 and 190182). All samples were de-identified
576 and written informed consent was obtained. Peripheral blood mononuclear cells were
577 isolated by ficoll gradient from unidentified healthy adult volunteers as previously
578 described.[50] A pathologist from the Vanderbilt Children's Hospital provided fresh
579 intestinal tissue specimens from infants. Isolation of human cells associated with the
580 intestinal epithelium was performed as previously described.[51] Briefly, tissue was cut in
581 small ~1 cm pieces and incubated with slow shaking for 30 minutes at room
582 temperature in HBSS (without calcium and magnesium) supplemented with 5% fetal
583 bovine serum, 5mM EDTA and an 1% antibiotic mix (pen-strep-AmphoB; Fisher-Lonza).
584 After incubation, cells in the supernatant were recovered.
585
586 *Reagents and flow cytometry.* Fluorochrome-coupled anti-mouse CD4, -CD44, -CD45, -
587 CD8α, -TCRβ, -TCR$\gamma\delta$, Ki69 and isotype controls were purchased from Thermofisher or
588 BD Biosciences. Annexin V and 7AAD were purchased from BD biosciences. All
589 staining samples were acquired using a FACS Canto II or 4-Laser Fortessa Flow
590 System (BD Biosciences) and data analyzed using FlowJo software (Tree Star). Cell
591 staining was performed following conventional techniques. Manufacturer's instructions
592 were followed for Annexin V staining. FACS sorting was performed using a FACSAria III
593 at the Flow Cytometry Shared Resource at VUMC.
594
595 *In vitro survival assay.* Total IEL enriched for $CD45^+$ cells using magnetic beads
596 (Miltenyi) or FACS-enriched subpopulations were incubated in a 96-well flat-bottom well
597 plate (Falcon, Fisher Scientific) at a density of $5x10^5$ cells/ml in RPMI containing 10%
598 fetal bovine serum. In some groups culture media was supplemented with anti-

599 osteopontin (2 μg/ml) (R&D), recombinant osteopontin (2 μg/ml) (R&D), or anti-CD44 (5
600 μg/ml)(Thermofisher). Cells were cultured in 5% CO_2 at 37^{o}C. At time 0 and every 24 h,
601 an aliquot from the culture was taken to count live cells. Percentage of live cells was
602 calculated in reference to time 0. For human samples, total PBMC or IEL were cultured
603 in the presence or absence of recombinant human osteopontin (2 μg/ml) (R&D) and
604 anti-human-CD44 (5 μg/ml) (Thermofisher).
605
606 *Transcription profile analysis.* For gene expression array, RNA was isolated from FACS-
607 enriched IEL subpopulations from 4 individual WT and Spp-1$^{-/-}$ mice. Samples were
608 prepared for RT^{2} Profiler PCR Array (QIAGEN PAMM-012Z) and analyzed following
609 manufacturer's instructions. For RNAseq analysis, RNA was isolated from FACS-
610 enriched CD45^{+} IEL derived from WT mice cultured for 24 h in the presence or absence
611 of recombinant osteopontin using the QIAGEN RNeasy micro kit. Sequencing was
612 performed on an Illumina NovaSeq 6000 (2 x 150 base pair, paired-end reads). The tool
613 Salmon [52] was used for quantifying the expression of RNA transcripts. The R project
614 software along with the edgeR method [53] was used for differential expression analysis.
615 For gene set enrichment analysis (GSEA), RNAseq data was ranked according to the t-
616 test statistic. The gene sets curated (C2), GO (C5), immunological signature collection
617 (C7) and hallmarks of cancer (H) of the Molecular Signatures Database (MSigDB) were
618 used for enrichment analysis. GSEA enrichment plots were generated using the GSEA
619 software [54] from the Broad Institute with 1000 permutations.
620
621 *Adoptive transfer of total T cells*. Total splenocytes from WT mice were depleted of
622 CD19-positive cells using magnetic beads (Miltenyi). Four to 6 million cells were
623 adoptively transferred (i.p.) into Rag-2$^{-/-}$ or Spp-1$^{-/-}$Rag-2$^{-/-}$ mice. Starting weight was
624 determined prior to injection. Seven or 28 days later, recipient mice were weighed,
625 sacrificed and donor cells from the intestines analyzed by flow cytometry. In some
626 experiments a segment of the colon was excised and prepared for histological
627 examination. In some experiments CD19-depleted splenocytes from CD44$^{-/-}$ mice were
628 adoptively transferred into Rag-2$^{-/-}$ or Spp-1$^{-/-}$Rag-2$^{-/-}$ mice. Mice were weighed weekly
629 for 4 weeks, and cells and colon analyzed as indicated above.

In vitro and in vivo Foxp3 expression. Lamina propria lymphocytes isolated from RFP-Foxp3 mice were cultured in the presence or absence of recombinant osteopontin and anti-CD44 antibodies as described above. At time 0 and 72 h later, cells were analyzed by flow cytometry to detect RFP expression in live $TCR^{+}CD4^{+}$ cells. For *in vivo* experiments, $CD4^{+}RFP^{+}$ splenocytes were enriched by FACS and 2 $x10^{5}$ cells were adoptively transferred i.p. into Rag-$2^{-/-}$ or Spp-$1^{-/-}$Rag-$2^{-/-}$ mice. Eight weeks later, IEL were isolated and RFP expression analyzed in $CD45^{+}TCR\beta^{+}CD4^{+}$ donor-derived cells.

Statistical analysis. Statistical significance between 2 groups was determined using Mann-Whitney U-test. For analysis of 3 groups or more, one-way nonparametric (Kruskal-Wallis) test or two-way ANOVA followed by Dunn's multiple comparison tests were used appropriately. All data was analyzed in GraphPad Prism 7 and showed as mean ± standard error mean (SEM). A *P* value <0.05 was considered significant.

Acknowledgments

We thank the Flow Cytometry Shared Resource for technical help and guidance; the Translational Pathology Shared Resource for tissue processing. We thank Dr. Luc Van Kaer for revising the manuscript. This work was supported by NIH grant R01DK111671 (to D.O-V.); Careers in Immunology Fellowship Program from the American Association of Immunologist (to D.O-V. and A.N.); National Library of Medicine T15 LM00745 grant (to M.J.G.); and scholarships from the Digestive Disease Research Center at Vanderbilt University Medical Center supported by NIH grant P30DK058404.

Author Contributions

A.N., designed and performed experiments, analyzed data and wrote the manuscript; M.J.G., designed and performed experiments, analyzed data and wrote the manuscript; K.L.H., performed experiments; M.B.P., provided expert pathological analysis of colon and small intestine tissue; J-H.W., provided procurement of human samples; D.O-V., designed and performed experiments, analyzed data, wrote the manuscript and procured funding.

References

1. Cheroutre, H., Lambolez, F. & Mucida, D. The light and dark sides of intestinal intraepithelial lymphocytes. *Nat Rev Immunol* **11**, 445-456 (2011).

2. Olivares-Villagomez, D. & Van Kaer, L. Intestinal Intraepithelial Lymphocytes: Sentinels of the Mucosal Barrier. *Trends Immunol* (2017).

3. Van Kaer, L. & Olivares-Villagomez, D. Development, Homeostasis, and Functions of Intestinal Intraepithelial Lymphocytes. *J Immunol* **200**, 2235-2244 (2018).

4. Fuchs, A. *et al.* Intraepithelial type 1 innate lymphoid cells are a unique subset of IL-12- and IL-15-responsive IFN-gamma-producing cells. *Immunity* **38**, 769-781 (2013).

5. Talayero, P. *et al.* Innate Lymphoid Cells Groups 1 and 3 in the Epithelial Compartment of Functional Human Intestinal Allografts. *Am J Transplant* **16**, 72-82 (2016).

6. Van Acker, A. *et al.* A Murine Intestinal Intraepithelial NKp46-Negative Innate Lymphoid Cell Population Characterized by Group 1 Properties. *Cell Rep* **19**, 1431-1443 (2017).

7. Ettersperger, J. *et al.* Interleukin-15-Dependent T-Cell-like Innate Intraepithelial Lymphocytes Develop in the Intestine and Transform into Lymphomas in Celiac Disease. *Immunity* **45**, 610-625 (2016).

8. Van Kaer, L. *et al.* CD8alphaalpha(+) Innate-Type Lymphocytes in the Intestinal Epithelium Mediate Mucosal Immunity. *Immunity* **41**, 451-464 (2014).

9. Edelblum, K.L. *et al.* gammadelta Intraepithelial Lymphocyte Migration Limits Transepithelial Pathogen Invasion and Systemic Disease in Mice. *Gastroenterology* **148**, 1417-1426 (2015).

10. Ismail, A.S. *et al.* Gammadelta intraepithelial lymphocytes are essential mediators of host-microbial homeostasis at the intestinal mucosal surface. *Proc Natl Acad Sci U S A* **108**, 8743-8748 (2011).

11. Inagaki-Ohara, K. *et al.* Mucosal T cells bearing TCRgammadelta play a protective role in intestinal inflammation. *J Immunol* **173**, 1390-1398 (2004).

12. Chen, Y., Chou, K., Fuchs, E., Havran, W.L. & Boismenu, R. Protection of the intestinal mucosa by intraepithelial gamma delta T cells. *Proc Natl Acad Sci U S A* **99**, 14338-14343 (2002).

13. Guy-Grand, D., DiSanto, J.P., Henchoz, P., Malassis-Seris, M. & Vassalli, P. Small bowel enteropathy: role of intraepithelial lymphocytes and of cytokines (IL-12, IFN-gamma, TNF) in the induction of epithelial cell death and renewal. *Eur J Immunol* **28**, 730-744 (1998).

14. Poussier, P., Ning, T., Banerjee, D. & Julius, M. A unique subset of self-specific intraintestinal T cells maintains gut integrity. *J Exp Med* **195**, 1491-1497 (2002).

15. Lepage, A.C., Buzoni-Gatel, D., Bout, D.T. & Kasper, L.H. Gut-derived intraepithelial lymphocytes induce long term immunity against Toxoplasma gondii. *J Immunol* **161**, 4902-4908 (1998).

16. Masopust, D. *et al.* Dynamic T cell migration program provides resident memory within intestinal epithelium. *J Exp Med* **207**, 553-564 (2010).

17. Masopust, D., Jiang, J., Shen, H. & Lefrancois, L. Direct analysis of the dynamics of the intestinal mucosa CD8 T cell response to systemic virus infection. *J Immunol* **166**, 2348-2356 (2001).

18. Das, G. *et al.* An important regulatory role for CD4+CD8 alpha alpha T cells in the intestinal epithelial layer in the prevention of inflammatory bowel disease. *Proc Natl Acad Sci U S A* **100**, 5324-5329. PMC1535703 (2003).

19. Kumar, A.A., Delgado, A.G., Piazuelo, M.B., Van Kaer, L. & Olivares-Villagomez, D. Innate CD8alphaalpha(+) lymphocytes enhance anti-CD40 antibody-mediated colitis in mice. *Immun Inflamm Dis* **5**, 109-123 (2017).

20. Franzen, A. & Heinegard, D. Isolation and characterization of two sialoproteins present only in bone calcified matrix. *Biochem J* **232**, 715-724 (1985).

21. Prince, C.W. *et al.* Isolation, characterization, and biosynthesis of a phosphorylated glycoprotein from rat bone. *J Biol Chem* **262**, 2900-2907 (1987).

22. Lund, S.A. *et al.* Osteopontin mediates macrophage chemotaxis via alpha4 and alpha9 integrins and survival via the alpha4 integrin. *J Cell Biochem* **114**, 1194-1202 (2013).

23. Ashkar, S. *et al.* Eta-1 (osteopontin): an early component of type-1 (cell-mediated) immunity. *Science* **287**, 860-864 (2000).

24. Hur, E.M. *et al.* Osteopontin-induced relapse and progression of autoimmune brain disease through enhanced survival of activated T cells. *Nat Immunol* **8**, 74-83 (2007).

25. Leavenworth, J.W., Verbinnen, B., Wang, Q., Shen, E. & Cantor, H. Intracellular osteopontin regulates homeostasis and function of natural killer cells. *Proc Natl Acad Sci U S A* **112**, 494-499 (2015).

26. Shinohara, M.L., Kim, H.J., Kim, J.H., Garcia, V.A. & Cantor, H. Alternative translation of osteopontin generates intracellular and secreted isoforms that mediate distinct biological activities in dendritic cells. *Proc Natl Acad Sci U S A* **105**, 7235-7239 (2008).

27. Oz, H.S., Zhong, J. & de Villiers, W.J. Osteopontin ablation attenuates progression of colitis in TNBS model. *Dig Dis Sci* **57**, 1554-1561 (2012).

28. Zhong, J., Eckhardt, E.R., Oz, H.S., Bruemmer, D. & de Villiers, W.J. Osteopontin deficiency protects mice from Dextran sodium sulfate-induced colitis. *Inflamm Bowel Dis* **12**, 790-796 (2006).

29. Sato, T. *et al.* Osteopontin/Eta-1 upregulated in Crohn's disease regulates the Th1 immune response. *Gut* **54**, 1254-1262 (2005).

30. Mishima, R. *et al.* High plasma osteopontin levels in patients with inflammatory bowel disease. *J Clin Gastroenterol* **41**, 167-172 (2007).

31. Gassler, N. *et al.* Expression of osteopontin (Eta-1) in Crohn disease of the terminal ileum. *Scand J Gastroenterol* **37**, 1286-1295 (2002).

32. Masuda, H., Takahashi, Y., Asai, S. & Takayama, T. Distinct gene expression of osteopontin in patients with ulcerative colitis. *J Surg Res* **111**, 85-90 (2003).

33. Neuman, M.G. Osteopontin biomarker in inflammatory bowel disease, animal models and target for drug discovery. *Dig Dis Sci* **57**, 1430-1431 (2012).

34. Boumans, M.J. *et al.* Safety, tolerability, pharmacokinetics, pharmacodynamics and efficacy of the monoclonal antibody ASK8007 blocking osteopontin in patients with rheumatoid arthritis: a randomised, placebo controlled, proof-of-concept study. *Annals of the rheumatic diseases* **71**, 180-185 (2012).

35. Ito, K. *et al.* The potential role of Osteopontin in the maintenance of commensal bacteria homeostasis in the intestine. *PLoS One* **12**, e0173629 (2017).

36. Weber, G.F., Ashkar, S., Glimcher, M.J. & Cantor, H. Receptor-ligand interaction between CD44 and osteopontin (Eta-1). *Science* **271**, 509-512 (1996).

37. Beura, L.K. *et al.* Normalizing the environment recapitulates adult human immune traits in laboratory mice. *Nature* **532**, 512-516 (2016).

38. Smolewski, P. & Robak, T. Inhibitors of apoptosis proteins (IAPs) as potential molecular targets for therapy of hematological malignancies. *Curr Mol Med* **11**, 633-649 (2011).

39. Kim, S., Shevde, N.K. & Pike, J.W. 1,25-Dihydroxyvitamin D3 stimulates cyclic vitamin D receptor/retinoid X receptor DNA-binding, co-activator recruitment, and histone acetylation in intact osteoblasts. *J Bone Miner Res* **20**, 305-317 (2005).

40. Olivares-Villagomez, D. & Van Kaer, L. TL and CD8alphaalpha: Enigmatic partners in mucosal immunity. *Immunol Lett* **134**, 1-6 (2010).

41. Olivares-Villagomez, D. *et al.* Thymus leukemia antigen controls intraepithelial lymphocyte function and inflammatory bowel disease. *Proc Natl Acad Sci U S A* **105**, 17931-17936. PMC2584730 (2008).

42. Bollyky, P.L. *et al.* CD44 costimulation promotes FoxP3+ regulatory T cell persistence and function via production of IL-2, IL-10, and TGF-beta. *J Immunol* **183**, 2232-2241 (2009).

43. Maki, K. *et al.* Interleukin 7 receptor-deficient mice lack gammadelta T cells. *Proc Natl Acad Sci U S A* **93**, 7172-7177. PMC38955 (1996).

44. Kennedy, M.K. *et al.* Reversible defects in natural killer and memory CD8 T cell lineages in interleukin 15-deficient mice. *J Exp Med* **191**, 771-780 (2000).

45. Montufar-Solis, D., Garza, T. & Klein, J.R. T-cell activation in the intestinal mucosa. *Immunol Rev* **215**, 189-201. PMC2754816 (2007).

46. Powrie, F., Correa-Oliveira, R., Mauze, S. & Coffman, R.L. Regulatory interactions between CD45RBhigh and CD45RBlow CD4+ T cells are important for the balance between protective and pathogenic cell-mediated immunity. *J Exp Med* **179**, 589-600. PMC2191378 (1994).

47. Powrie, F. *et al.* Inhibition of Th1 responses prevents inflammatory bowel disease in scid mice reconstituted with CD45RBhi CD4+ T cells. *Immunity* **1**, 553-562 (1994).

48. Kanayama, M. *et al.* Skewing of the population balance of lymphoid and myeloid cells by secreted and intracellular osteopontin. *Nat Immunol* **18**, 973-984 (2017).

49. Farrokhi, V., Chabot, J.R., Neubert, H. & Yang, Z. Assessing the Feasibility of Neutralizing Osteopontin with Various Therapeutic Antibody Modalities. *Sci Rep* **8**, 7781 (2018).

50. Hoek, K.L. *et al.* A cell-based systems biology assessment of human blood to monitor immune responses after influenza vaccination. *PLoS One* **10**, e0118528 (2015).

51. Weitkamp, J.H. *et al.* Necrotising enterocolitis is characterised by disrupted immune regulation and diminished mucosal regulatory (FOXP3)/effector (CD4, CD8) T cell ratios. *Gut* **62**, 73-82 (2013).

52. Patro, R., Duggal, G., Love, M.I., Irizarry, R.A. & Kingsford, C. Salmon provides fast and bias-aware quantification of transcript expression. *Nature methods* **14**, 417-419 (2017).

53. Robinson, M.D., McCarthy, D.J. & Smyth, G.K. edgeR: a Bioconductor package for differential expression analysis of digital gene expression data. *Bioinformatics* **26**, 139-140 (2010).

54. Subramanian, A. *et al.* Gene set enrichment analysis: a knowledge-based approach for interpreting genome-wide expression profiles. *Proc Natl Acad Sci U S A* **102**, 15545-15550 (2005).

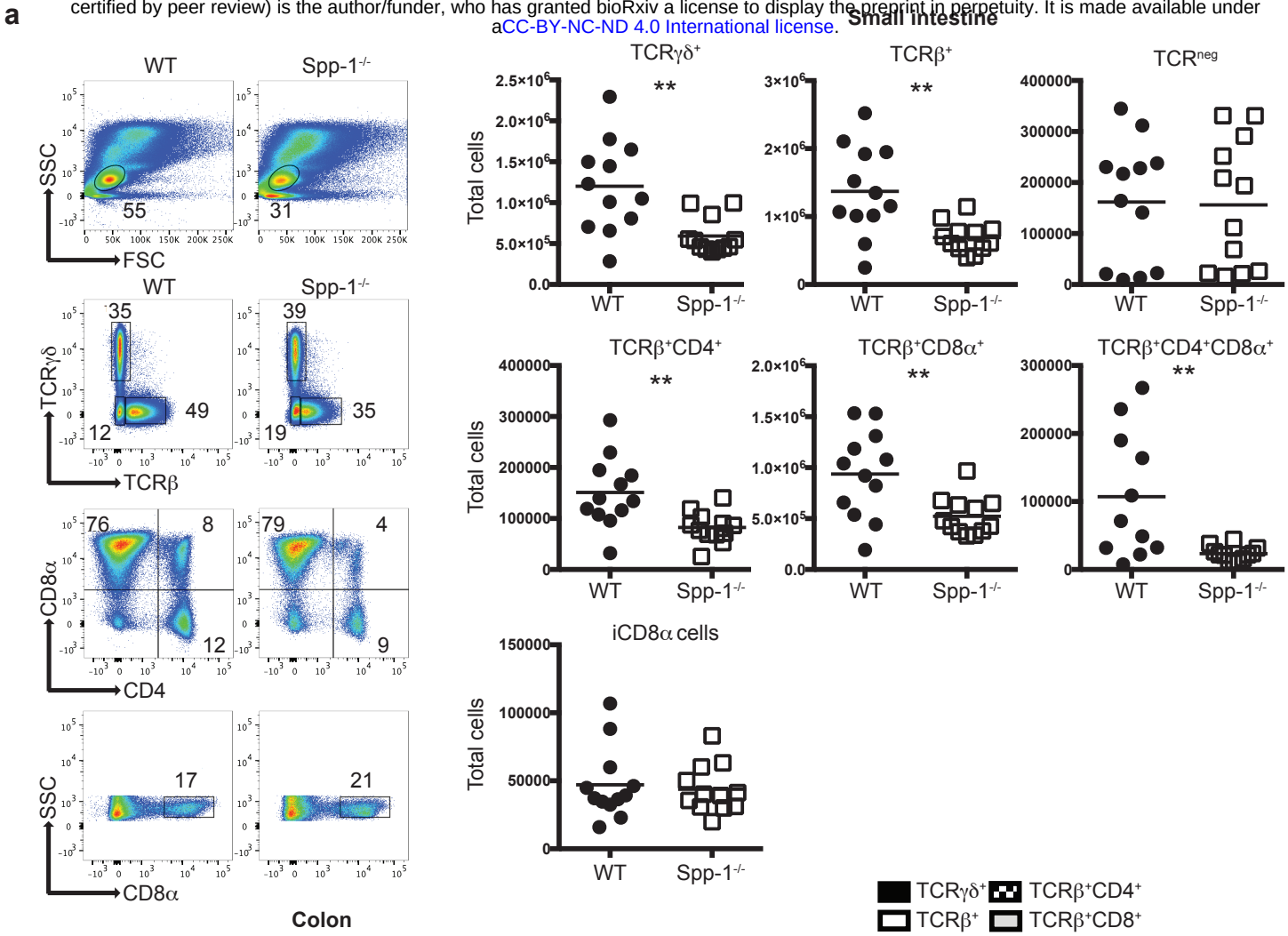

Figure 1

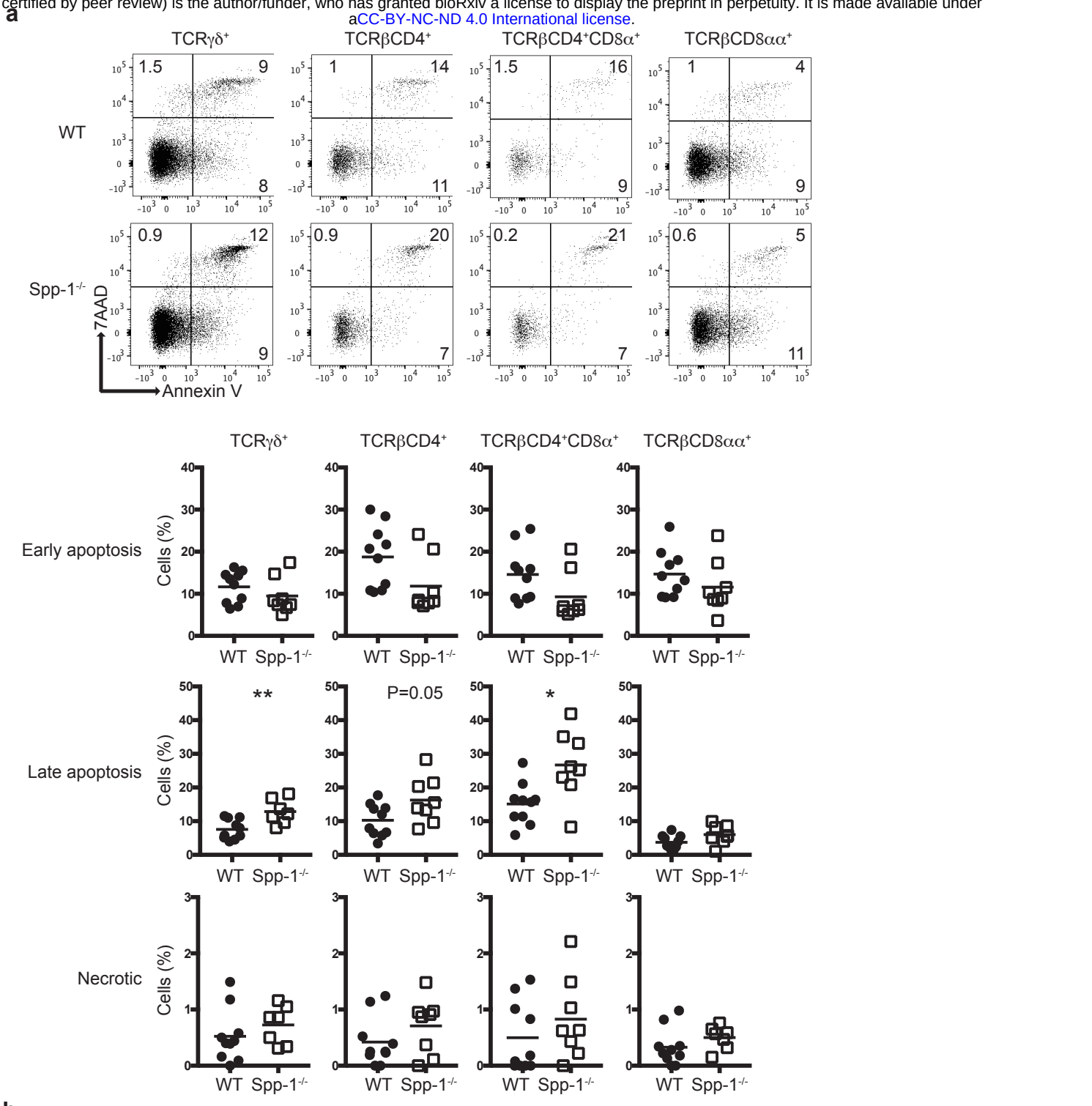

Figure 2

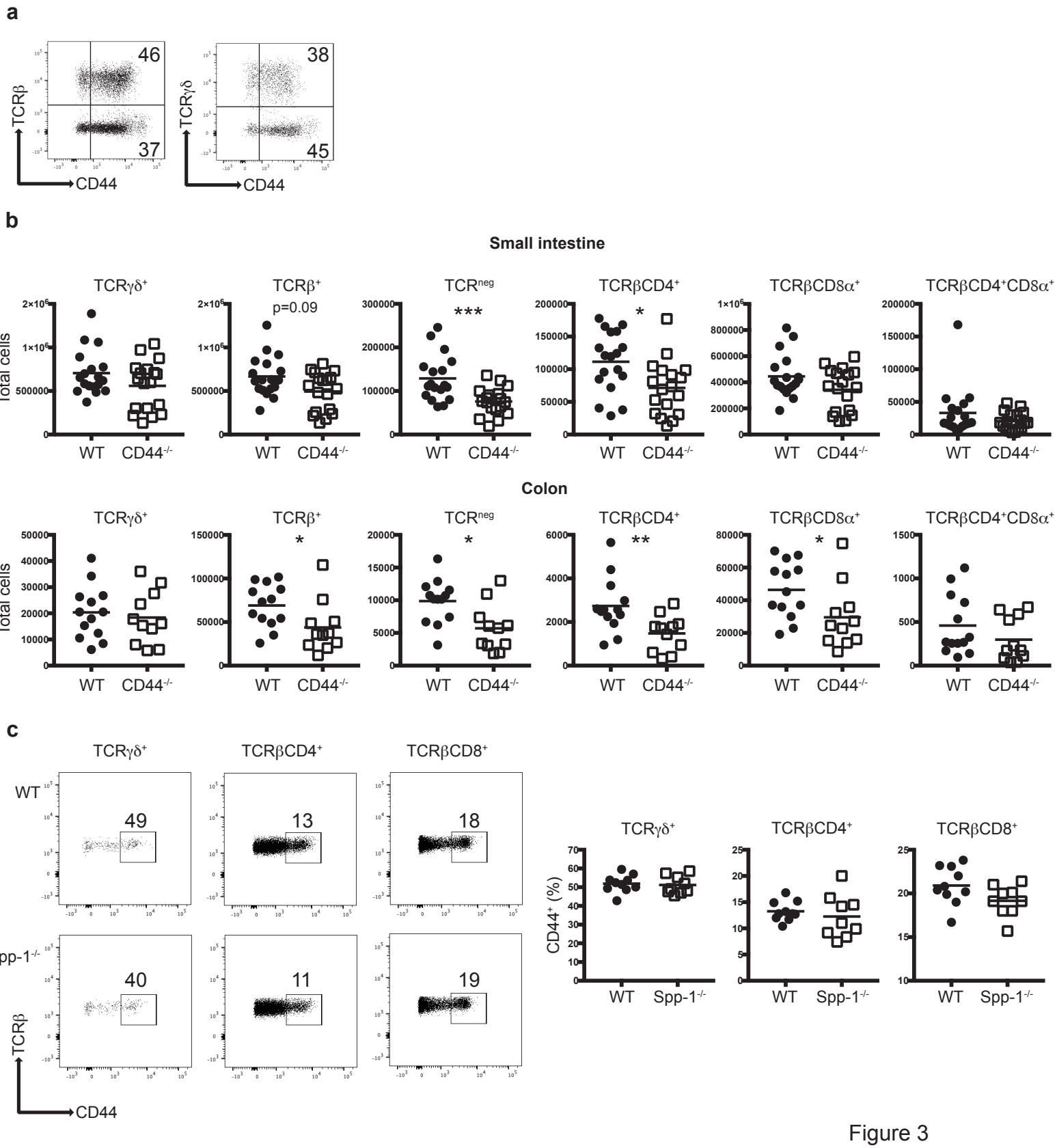

Figure 3

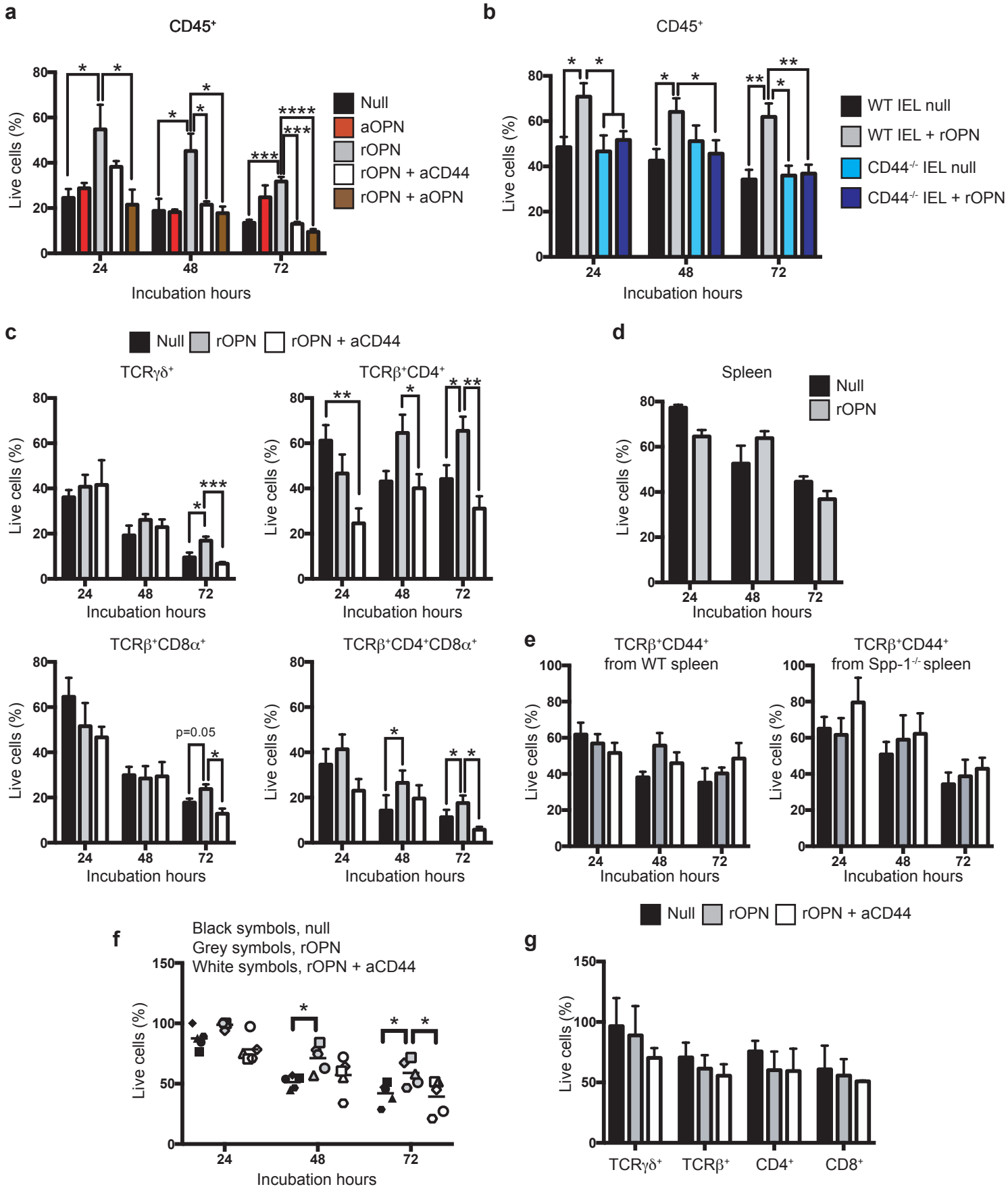

Figure 4

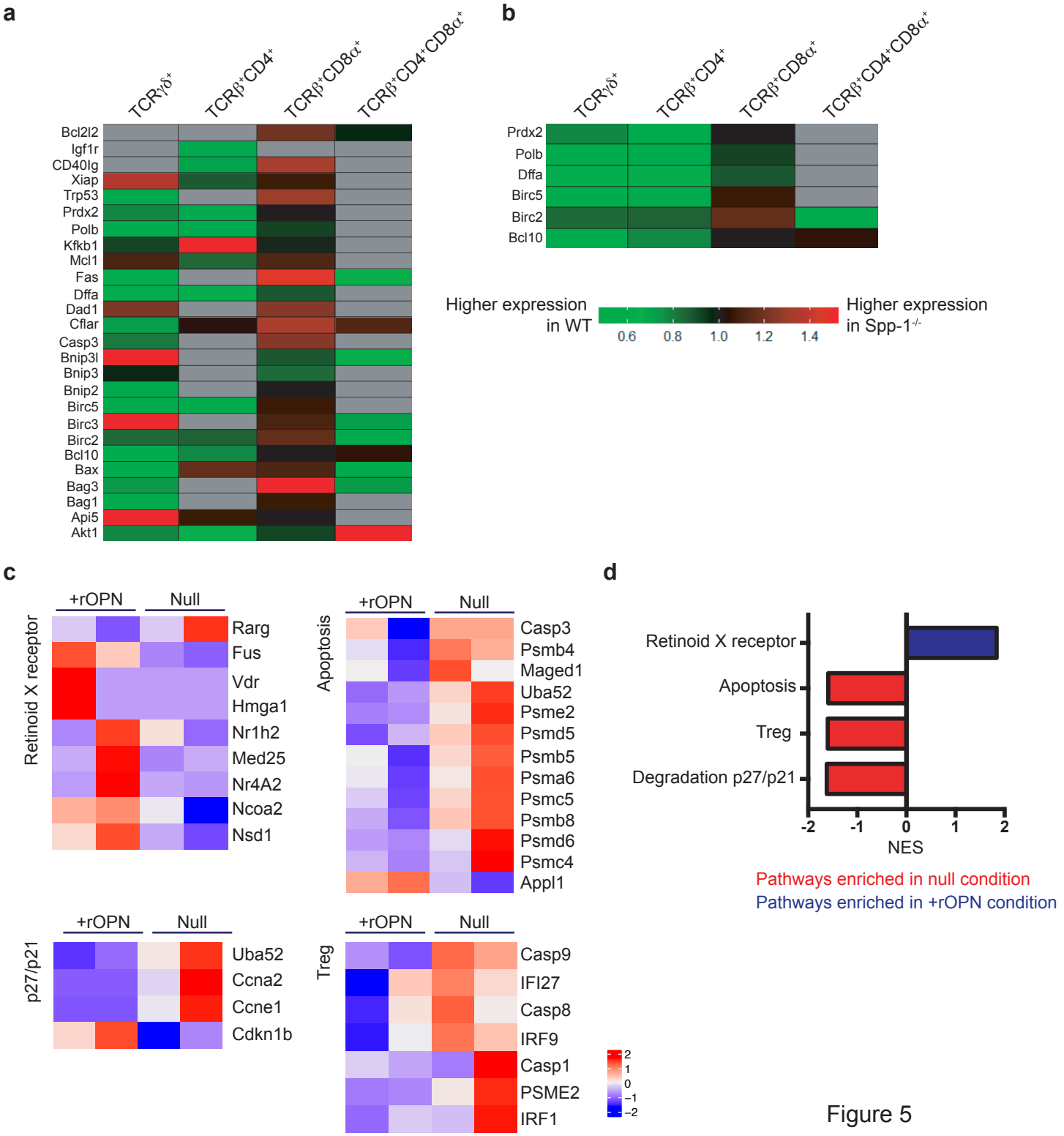

Figure 5

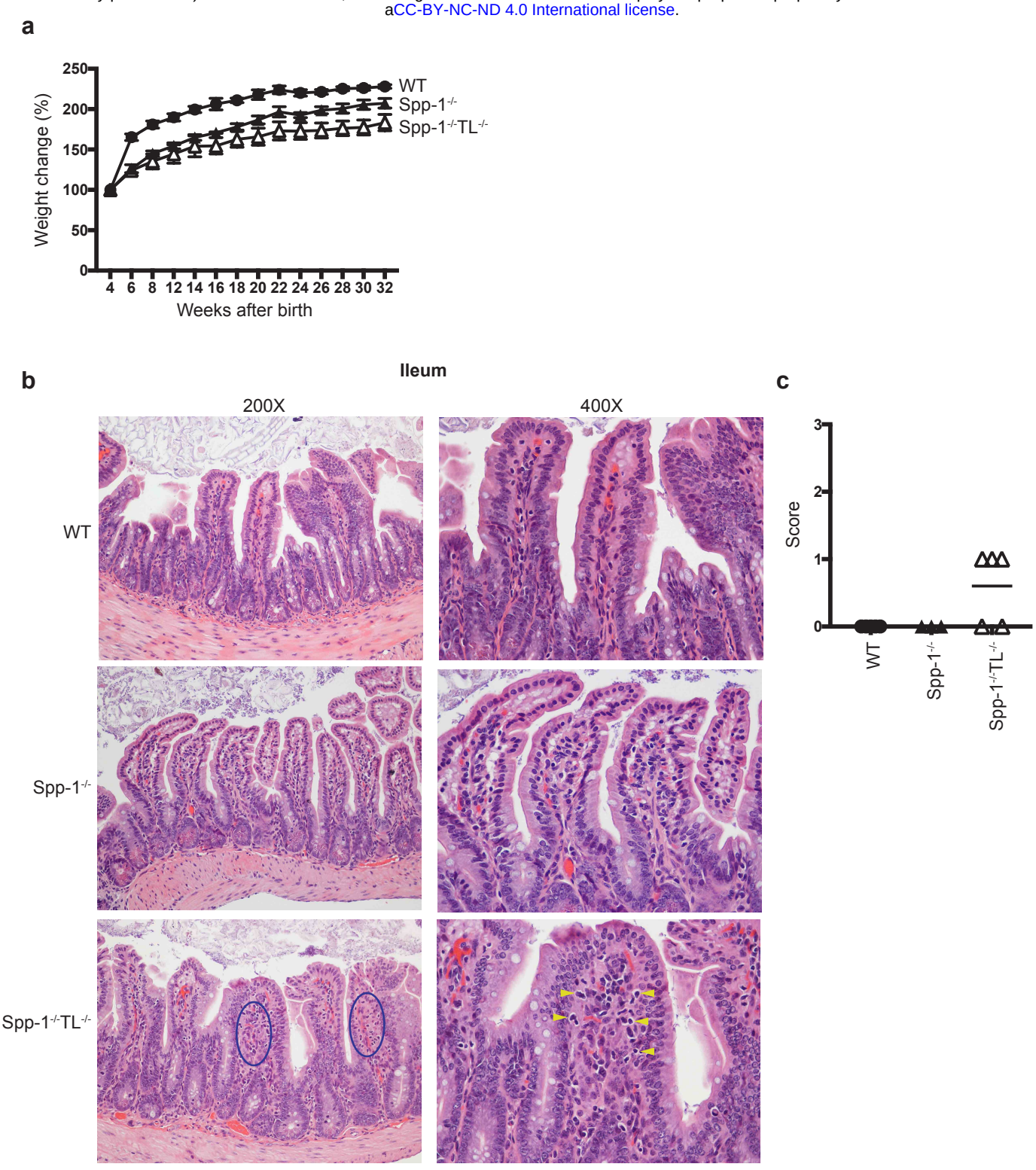

Figure 6

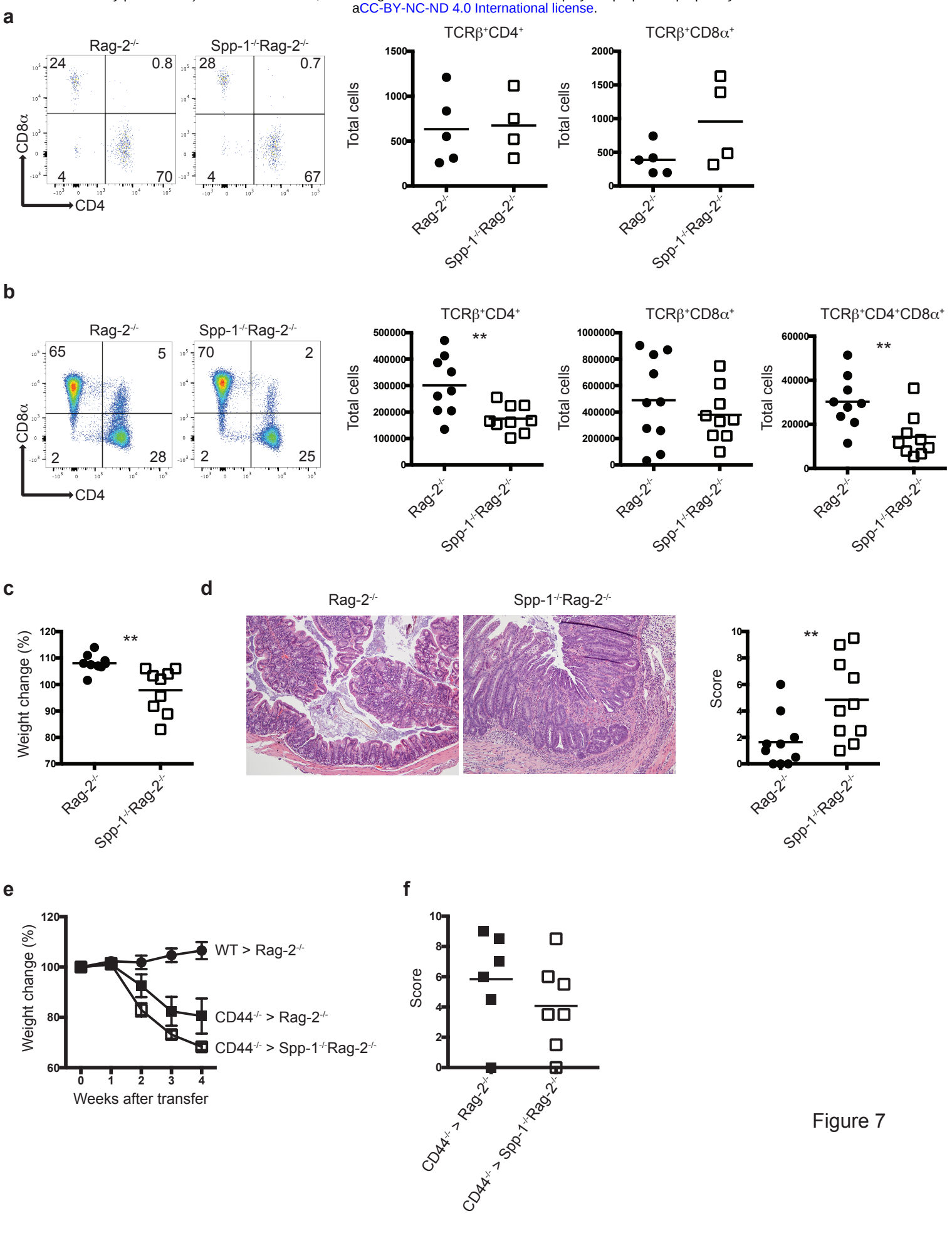

Figure 7

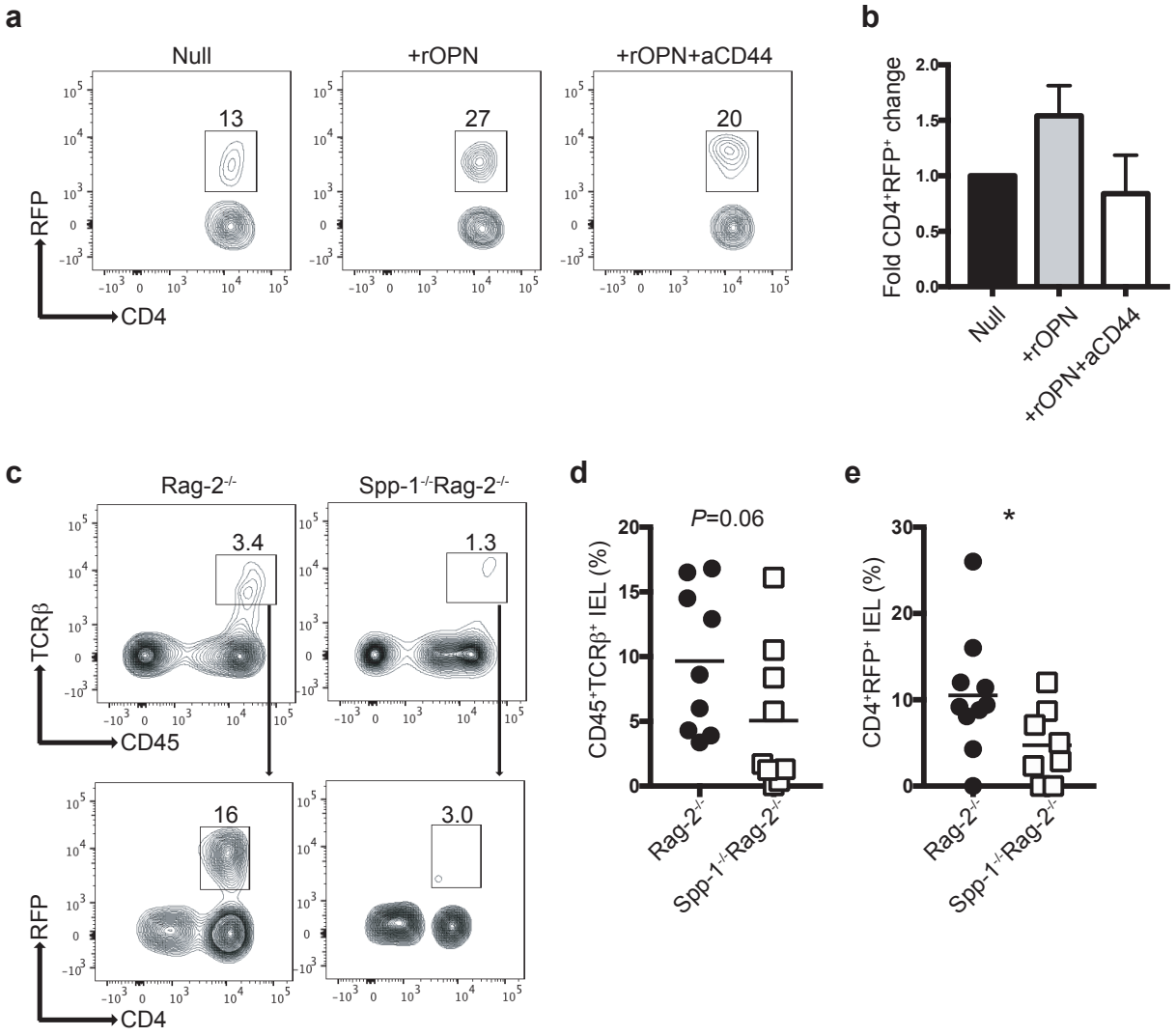

Figure 8